Supplementary Information

High Detectivity Ternary Near-Infrared Organic Photodetectors Based on Double Electron Transport Layer for Health Monitoring

Jingchong Liang[a,b], Honglin Wang[a,b], Zhangmin Yin[a,b], Mengwei Jia[a,b], Minghao Wang[a,b], Dawei Yan[c], Xiaoya Hou*[a,b] , and Jie Zhang[a,b]

a School of Mechanical Engineering, Jiangnan University, Wuxi 214122, People's Republic of China
b Jiangsu Key Laboratory of Advanced Food Manufacturing Equipment and Technology, Jiangnan University, Wuxi 214122, People's Republic of China
c School of Internet of Things Engineering, Jiangnan University, Wuxi 214122, People's Republic of China

Supplementary Figures

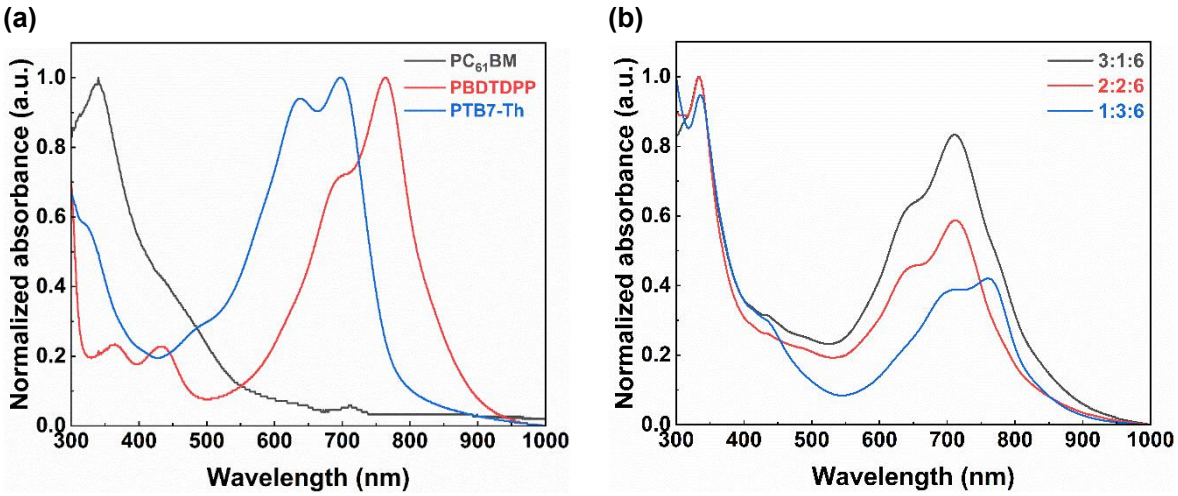

Fig. S1. Absorption spectra of (a) pure-film, and (b) ternary blend films with different D_1:D_2:A ratios.

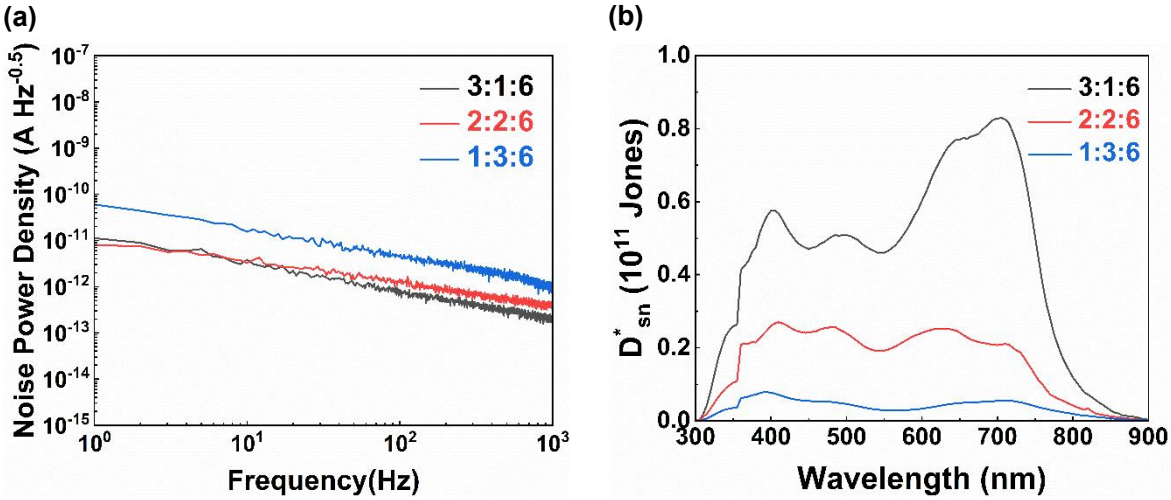

Fig. S2. (a) S_n and (b) D^*_{sn} of devices at −0.1V.

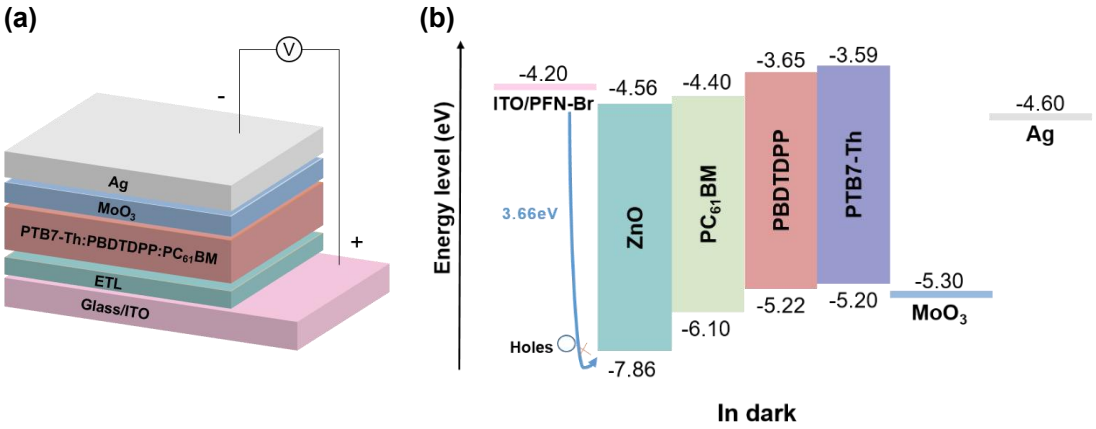

Fig. S3. (a) Device architecture of the different ETL devices. (b) Energy levels of the PFN-Br/ZnO device.

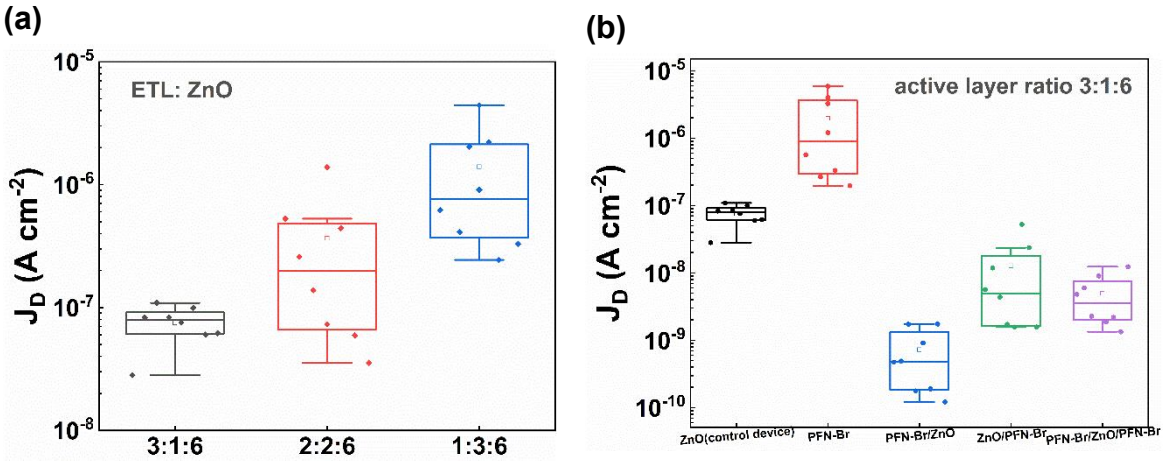

Fig. S4. The boxplot of J_D of OPDs: (a) with different active layer ratios using ZnO as the ETL, and (b) with different ETL at an active layer ratio of 3:1:6 under −0.1 V bias.

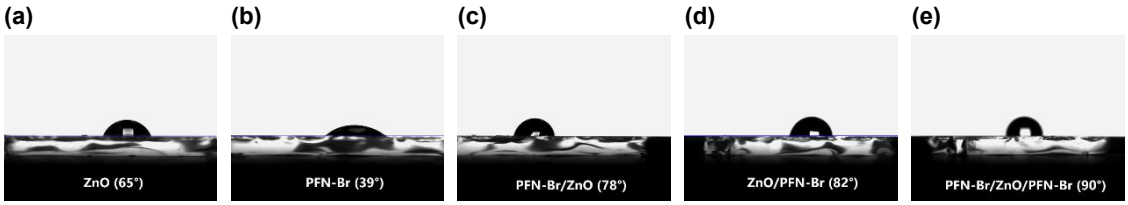

Fig. S5. Contact angles of different ETLs. (a) ZnO, (b) PFN-Br, (c) PFN-Br/ZnO, (d) ZnO/PFN-Br and (e) PFN-Br/ZnO/PFN-Br.

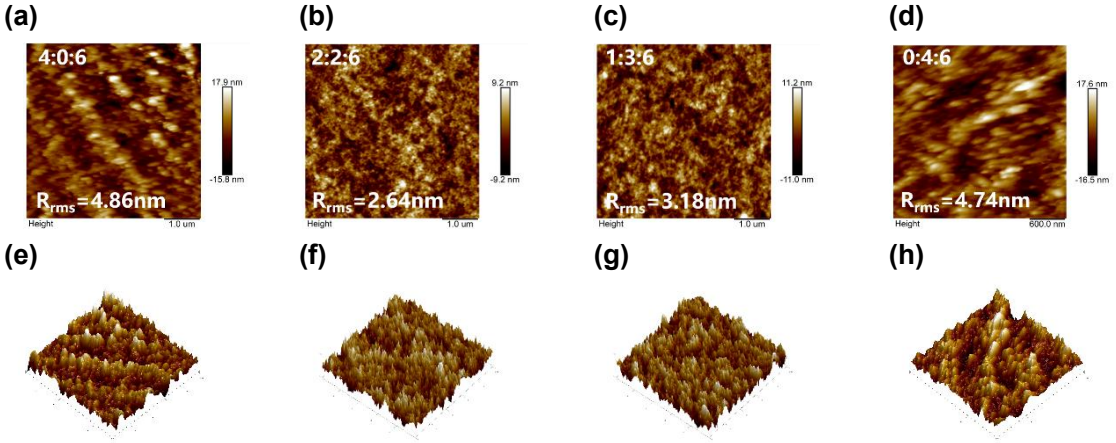

Fig. S6. AFM height images of the active layer on the (a) 4:0:6 device, (b) 2:2:6 device, (c) 1:3:6 device and (d) 0:4:6 device. 3D AFM diagrams of active layer on the (e) 4:0:6 device, (f) 2:2:6 device, (g) 1:3:6 device, and (h) 0:4:6 device.

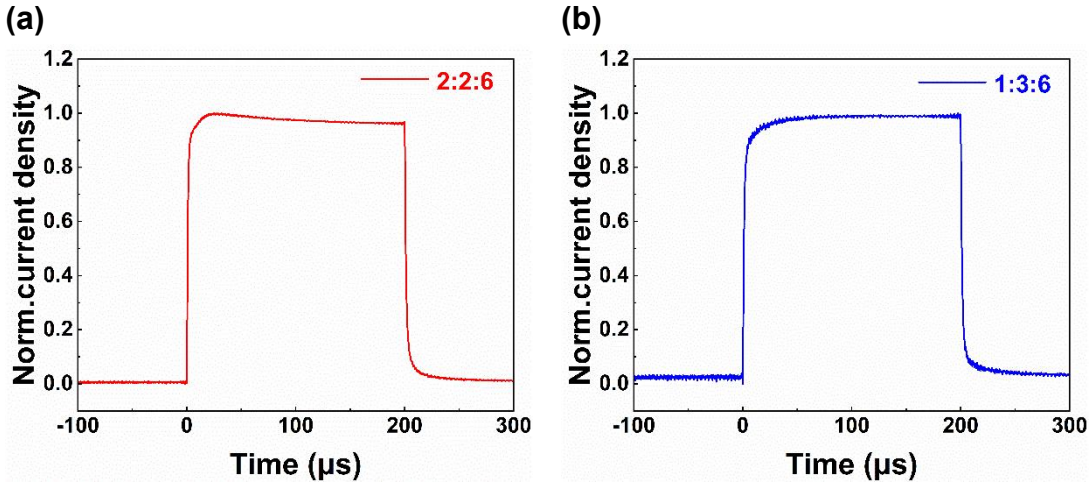

Fig. S7. TPC curves of the (a) 2:2:6 device and (b) 1:3:6 device.

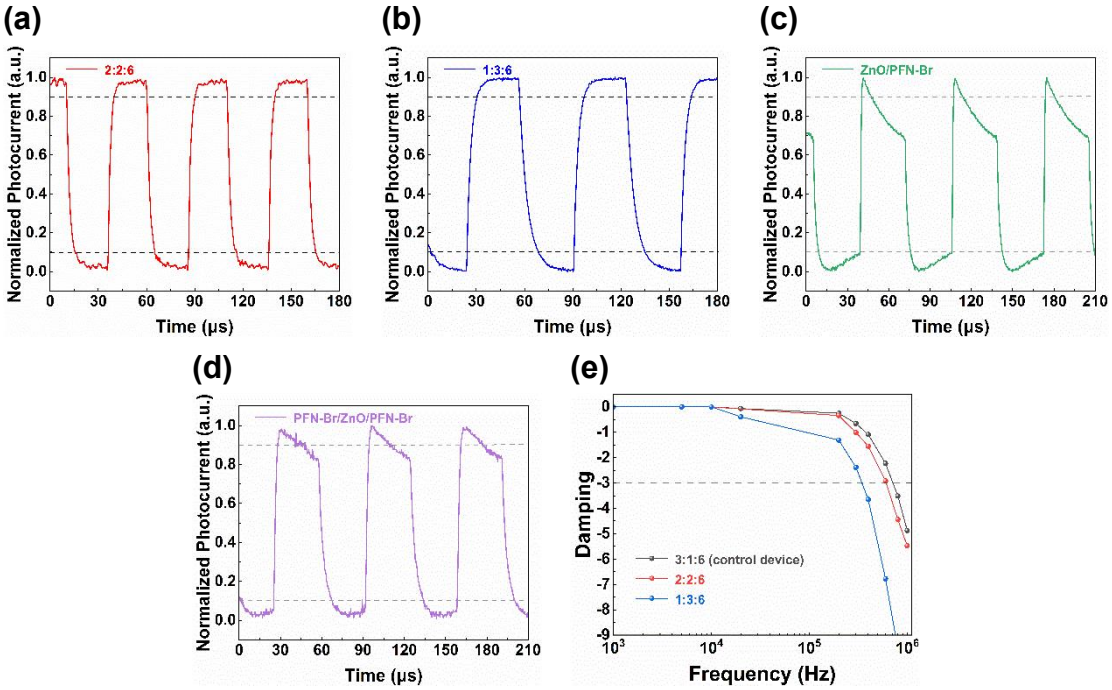

Fig. S8. Transient response of the (a) 2:2:6 device (b) 1:3:6 device (c) ZnO/PFN-Br device (d) PFN-BrZnO/PFN-Br device under the illumination of 705 nm LED. (e) f_{-3dB} curves of different D_1:D_2:A ratio devices at 0 V under white light irradiation of 100 mW cm^{-2} LED.

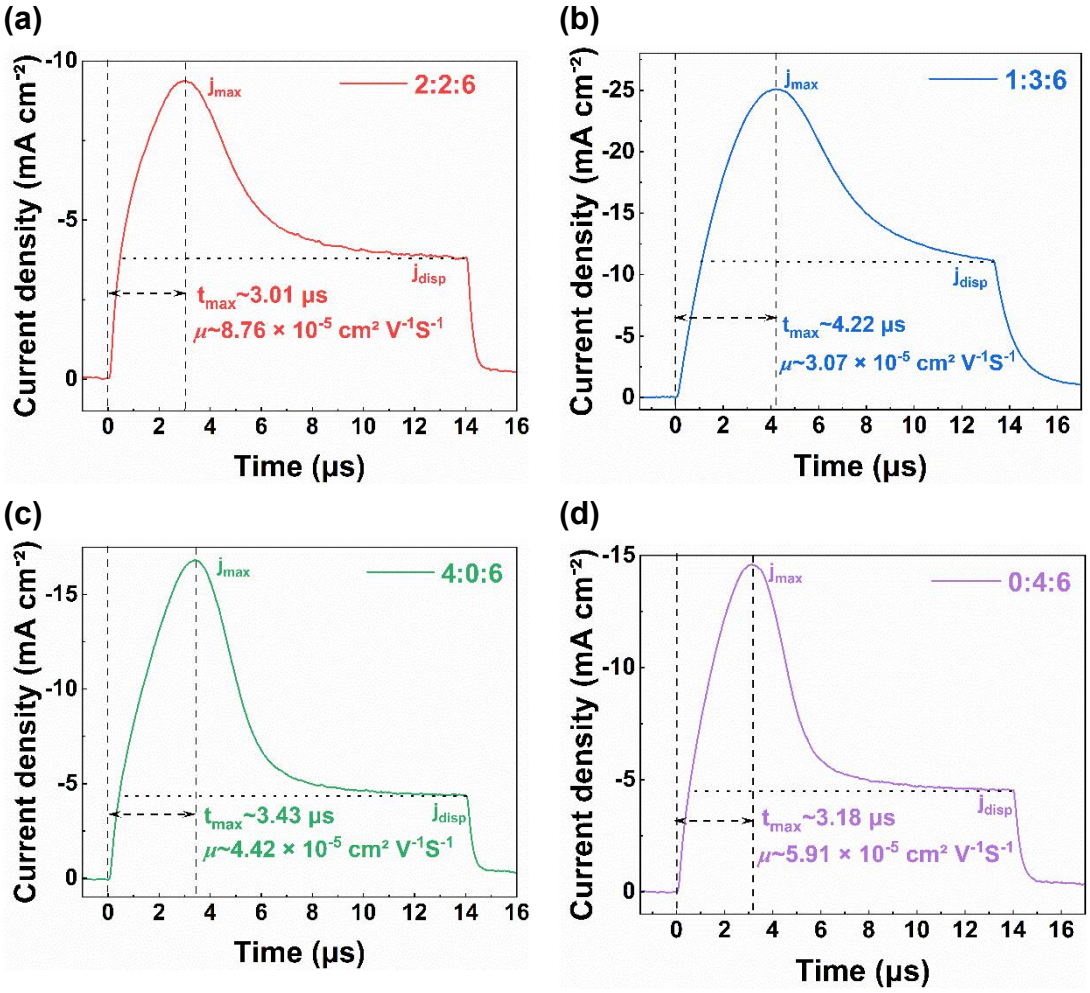

Fig. S9. Photo-CELIV curves of the (a) 2:2:6 device (b) 1:3:6 device (c) 4:0:6 device and (d) 0:4:6 device.

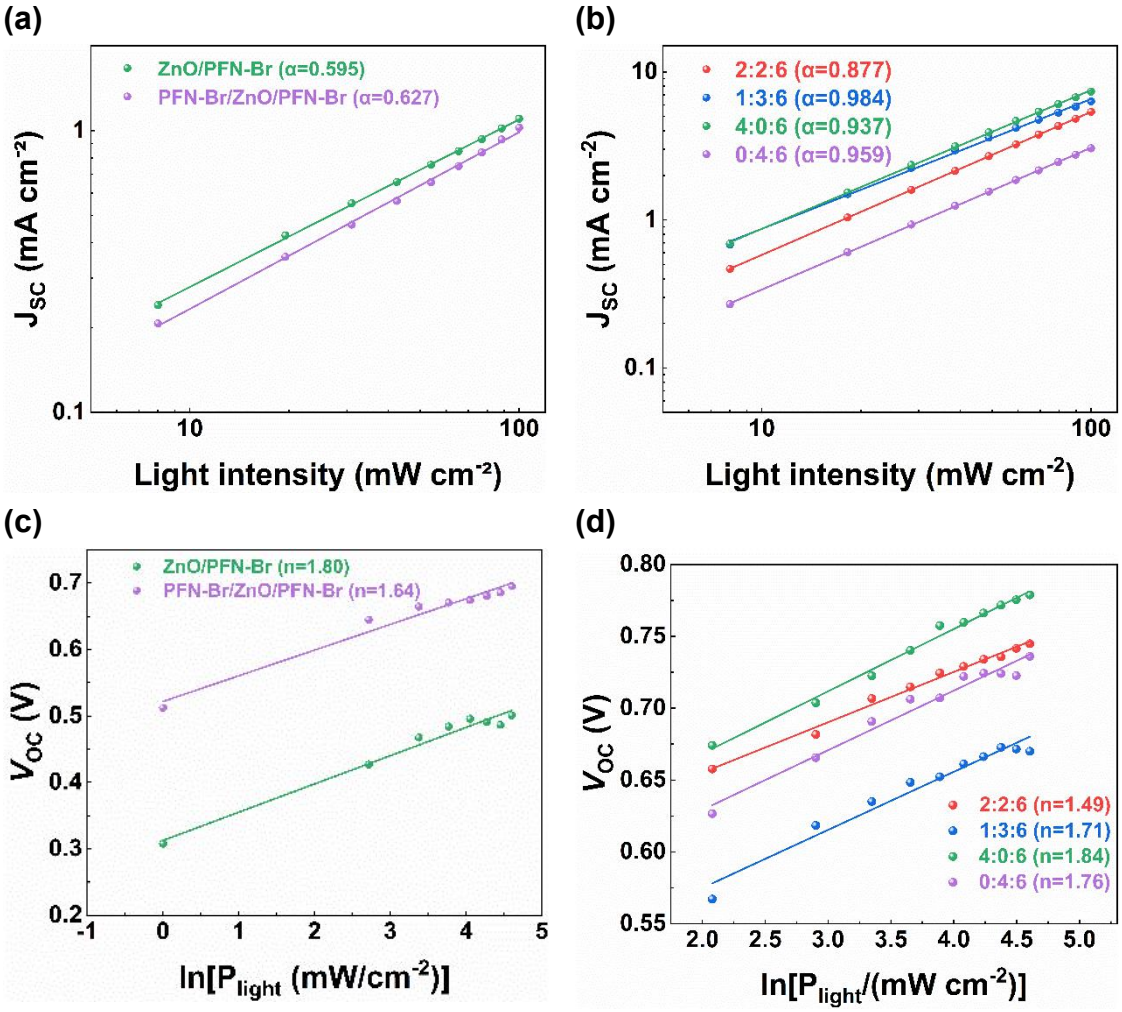

Fig. S10. J_{SC}–P_{light} curves of the (a) ZnO/PFN-Br, PFN-Br/ZnO/PFN-Br devices and (b) 2:2:6, 1:3:6, 4:0:6, and 0:4:6 devices. V_{oc}–P_{light} curves of the (c) ZnO/PFN-Br, PFN-Br/ZnO/PFN-Br devices and the (e) 2:2:6, 1:3:6, 4:0:6 and 0:4:6 devices.

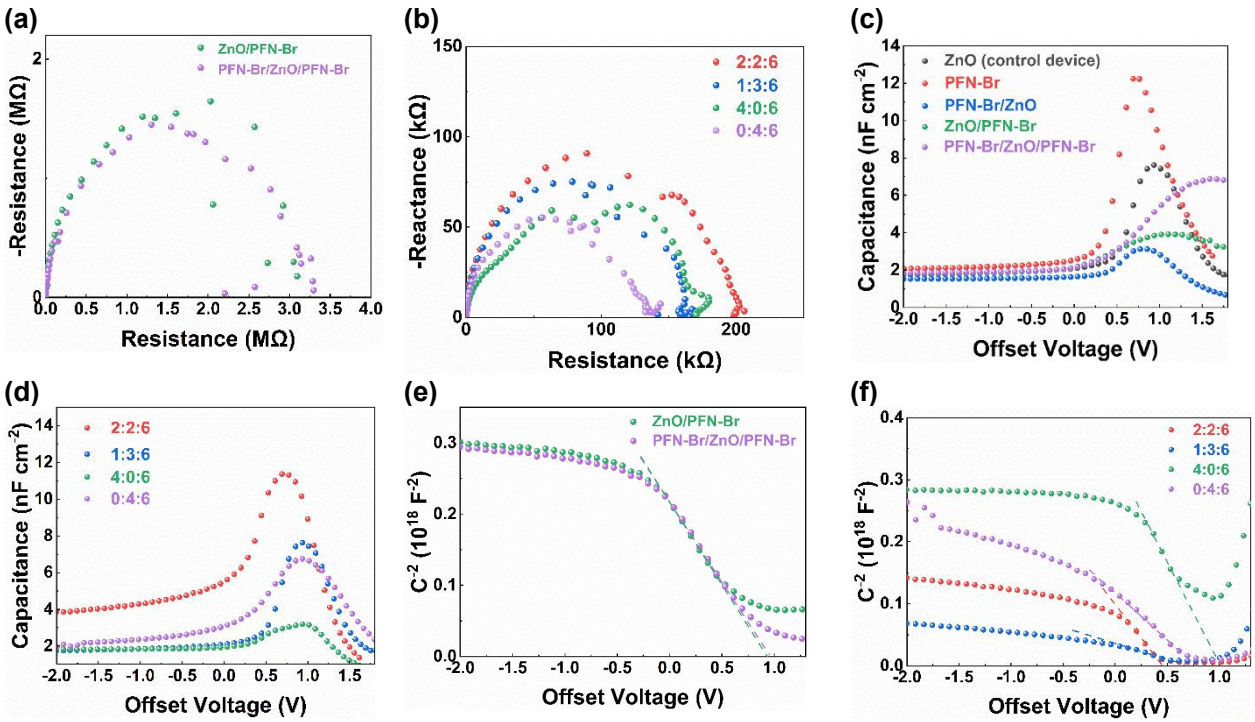

Fig. S11. Nyquist curves of the (a) ZnO/PFN-Br, PFN-Br/ZnO/PFN-Br devices, (b) 2:2:6, 1:3:6, 4:0:6 and 0:4:6 devices. *C*−*V* curves of the (c) different ETL devices and the (d) 2:2:6, 1:3:6, 4:0:6 and 0:4:6 devices. $1/C^2$−*V* characteristic curves (dashed line indicates linear fit) of the (e) ZnO/PFN-Br, PFN-Br/ZnO/PFN-Br devices and (f) 2:2:6, 1:3:6, 4:0:6 and 0:4:6 devices.

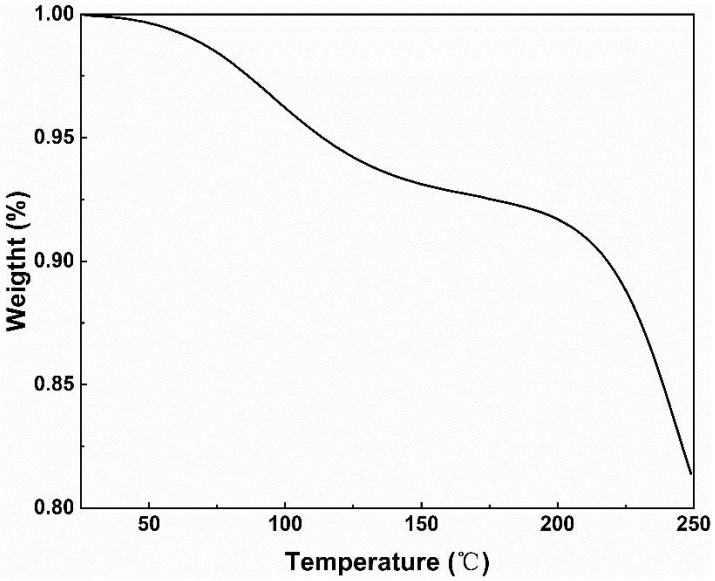

Fig. S12. TGA curve of PFN-Br.

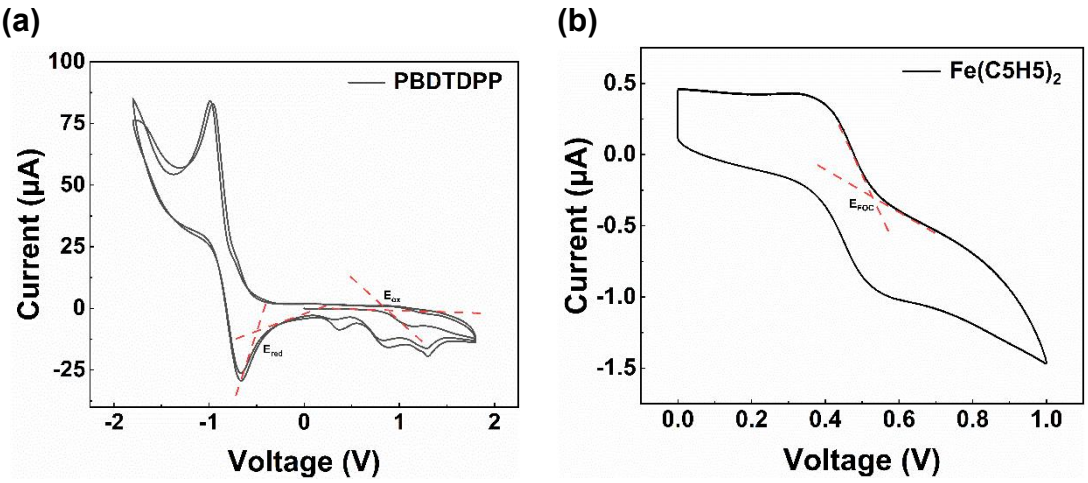

Fig. S13. Cyclic voltammogram of PBDTDPP in acetonitrile solution. $HOMO = -4.8 + E_{Foc} - E_{ox}$ (eV); $LUMO = -4.8 + E_{Foc} - E_{red}$ (eV).[1]

The *HOMO* (−5.22 eV) and *LUMO* (−3.65 eV) of PBDTDPP was tested using cyclic voltammetry.

Table S1. Main performance parameters of OPDs with different active layer ratios at 705 nm.

Device (D_1:D_2:A)	Bias [V]	J_D [A cm^{-2}]	*EQE* [%]	*R* [A W^{-1}]	D^*_{shot} [Jones]
3:1:6	−0.1	2.81×10^{-8}	32.6	0.186	1.95×10^{12}
2:2:6	−0.1	3.54×10^{-8}	17.3	0.098	8.89×10^{11}
1:3:6	−0.1	3.30×10^{-7}	10.8	0.061	1.85×10^{11}
4:0:6	−0.1	1.44×10^{-7}	32.8	0.187	8.01×10^{11}
0:4:6	−0.1	2.91×10^{-7}	4	0.023	6.81×10^{10}

Table S2. Summary of performance parameters of recent high-performance OPDs

Device Structure	*R* [A W^{-1}]	J_D [A cm^{-2}]	D^*_{shot} [Jones]	D^*_{sn} [Jones]	Ref
ITO/ZnO/P3HT: IDT-BOC/MoO_3/Ag	0.29 (560 nm)	4.91×10^{-6}	1.34×10^{11}	/	[2]
ITO/ZnO/TQ-3T: IEICO-4F/MoO_3/Ag	0.05 (1200 nm)	2.3×10^{-6}	/	1.03×10^{10}	[3]
ITO/PEDOT:PSS/PM6: Y6/PDINN/Ag	0.50 (830 nm)	7.07×10^{-10}	3.35×10^{13}	/	[4]
ITO/PEDOT:PSS/ D18:Y6/Phen-NaDPO/ Ag	0.68 (850 nm)	1.28×10^{-9}	6.35×10^{13}	6.80×10^{10}	[5]
ITO/ZnO/PM6: ABTPV-S/MoO_3/Ag	0.41 (820 nm)	1.80×10^{-9}	1.73×10^{13}	5.22×10^{11}	[6]
ITO/PEDOT: PSS/ PTB7-Th: COTCN2[a)]/C60-bissalt/ Al	0.23 (1000 nm)	1.08×10^{-7}	1.18×10^{12}	1.33×10^{11}	[7]
ITO/ZnO/PTQ10:IDSe/ MoO_3/Ag	0.37 (770 nm)	1.65×10^{-9}	/	3×10^{12}	[8]

ITO/Co_3O_4/P3HT:$PC_{61}BM$/Al	0.3 (600 nm)	2.5×10^{-9}	1.08×10^{13}	/	[9]
ITO-CI/CD1:PBN-14/LiF/Al	0.304 (670 nm)	9.03×10^{-10}	1.79×10^{13}	2.31×10^{12}	[10]
ITO/ZnO/PM6:PDTTIC-4F/MoO_3/Ag	0.55 (900 nm)	1.64×10^{-9}	2.40×10^{13}	/	[11]
ITO/PFN-Br/ZnO/PTB7-Th:PBDTDPP:$PC_{61}BM$/MoO_3/Ag	0.203 (705 nm)	4.72×10^{-10}	1.65×10^{13}	2.97×10^{11}	**This work**

Table S3. Parameters derived from photo-celiv curves and charge recombination analysis.

Device (D_1:D_2:A)	J_{max} [mA cm^{-2}]	μ [cm^{-3}]	α	n
3:1:6 (control device)	−12.4	1.14×10^{-4}	0.967	1.33
2:2:6	−9.37	8.76×10^{-5}	0.877	1.49
1:3:6	−25.1	3.07×10^{-4}	0.984	1.71
4:0:6	−16.8	4.42×10^{-5}	0.937	1.84
0:4:6	−14.5	5.91×10^{-5}	0.959	1.76

Table S4. Parameters of Mott–Schottky analysis and Nyquist curves.

Device (D_1:D_2:A)	N_A [cm^{-3}]	W [nm, −0.1V]	R_{sh} [MΩ]
3:1:6 (control device)	1.56×10^{16}	134	0.59
2:2:6	3.12×10^{16}	76	0.2
1:3:6	1.24×10^{17}	45	0.16
4:0:6	2.58×10^{16}	116	0.17
0:4:6	4.64×10^{16}	78	0.14

References

[1] T.-Y. Wu, R.-B. Sheu and Y. Chen, *Macromolecules*, 2004, **37**, 725–733.

[2] L. Lv, J. Yu, X. Sui, J. Wu, X. Dong, G. Lu, X. Liu, A. Peng, and H. Huang, *J. Mater. Chem. C.* , 2019, **7**, 5739-5747.

[3] P. Jacoutot, A. D. Scaccabarozzi, D. Nodari, J. Panidi, Z. Qiao, A. Schiza, A. D. Nega, A. Dimitrakopoulou-Strauss, V. G. Gregoriou, M. Heeney, C. L. Chochos, A. A. Bakulin and N. Gasparini, *Sci. Adv.*, 2023, **9**, eadh2694.

[4] Z. Yang, B. G. Kim, W. Jang and D. H. Wang, *J. Mater. Chem. C*, 2024, **12**, 3261–3271.

[5] W. Xu, Y. Gao, K. Qian, B. Wang, R. Xu, M. He, T. Li, G. Xing, S. Yang and G. Wei, *J. Mater. Chem. C*, 2022, **10**, 9391–9400.

[6] Z. Zhong, X. Liu, L. Li, Z. Han, Y. He, X. Xu, J. Hai, R. Zhu and J. Yu, *Sci. China Chem.*, 2023, **66**, 242–250.

[7] J. Ha, H. J. Eun, B. Park, H. Ahn, D. R. Hwang, Y. S. Shim, J. Heo, C. Lee, S. C. Yoon, J. H. Kim and S. Ko, *Adv Funct Materials*, 2023, **33**, 2211486.

[8] Z. Qiao, Q. He, A. D. Scaccabarozzi, J. Panidi, A. Marsh, Y. Han, P. Jacoutot, D. Nodari, T. Zhang, A. Way, A. J. P. White, T. D. Anthopoulos, W. C. Tsoi, A. A. Bakulin, M. Heeney, Z. Fei and N. Gasparini, *J. Mater. Chem. C*, 2024, **12**, 5766–5775.

[9] K. Lu, Y. Gao, Z. Wang, X. Wang and H. Meng, *J. Mater. Chem. C*, 2023, **11**, 8600–8608.

[10] J. Wang, R. Zhao, L. Zhang, J. Miao, J. Liu and L. Wang, *J. Mater. Chem. C*, 2023, **11**, 14421–14428.

[11] Y. Chen, Y. Zheng, Y. Jiang, H. Fan and X. Zhu, *J. Am. Chem. Soc.*, 2021, **143**, 4281–4289.